Physica Scripta. Vol. T80, 351–353, 1999

Double Ionization of Helium by Fast Fully Stripped Ions

B. Bapat,[1] R. Moshammer,[1] W. Schmitt,[2] H. Kollmus,[1] R. Mann,[2] R. Dörner,[3] Th. Weber,[3] K. Khayyat,[3] A. Cassimi,[4] L. Adoui,[4] J. P. Grandin[4] and J. Ullrich[1]

[1]Fakultät für Physik, Universität Freiburg, 79104 Freiburg, Germany
[2]Gesellschaft für Schwerionenforschung, 64291 Darmstadt, Germany
[3]Institut für Kernphysik, Universität Frankfurt, 60486 Frankfurt, Germany
[4]CIRIL, 14040 Caen, France

Received September 14, 1998; accepted in revised form November 19, 1998

PACS Ref: 31.80+x,34.50Fa

Abstract

A complete momentum-space map of the double ionisation events in the collision of 100 MeV/u C^{6+} ions with helium has been obtained. From this map the angular distribution of two ejected electrons is generated as a function of the momentum transferred by the projectile to the atom. Analysis of the angular distribution of the fragments in the plane transverse to the projectile axis (the azimuthal plane) shows a separation of events into two domains, depending on the momentum transferred by the projectile to the target. For momentum transfers smaller than 1.2 a.u., both electrons are distributed independent of the azimuthal angle. For momentum transfers larger than 1.2 a.u., the electron with larger energy is distinctly emitted along the direction of momentum transfer, and the one with smaller energy is distributed isotropically. The value of 1.2 a.u. is approximately equal to the mean value of the momenta of the bound electrons in the helium atom and demarcates indirect, soft collisions and direct, hard collisions respectively. For soft collisions, the electron angular distribution shows certain similarities with the angular distributions in photo-double ionization.

1. Introduction

The question whether there are similarities between ionization brought about by ion-impact and by the absorption of one or more photons has been addressed often in the past. Indeed, for very high projectile velocities, Weizsäcker [1] and Williams [2] showed long ago that ionization of atoms by ions could be regarded as absorption of virtual photons with a range of wavelengths. Following the Bethe-Born approximation [3], Kim and Inokuti [4] expressed the cross sections for ionization by charged particles in terms of the generalized oscillator strengths, a concept related to the response of an atom in a photon field.

A widely investigated aspect of double ionization of helium is the variation of the ratio R of double-to-single ionization cross sections, for charged particle impact ionization, and to a lesser extent for photoionization. Similarities between R for the two types of ionization have been suggested, based on the momentum transfer to the target [5,6]. There has been no experimental confirmation of these equivalences. Recently, Moshammer *et al.* [7] demonstrated the equivalence of photoabsorption with the impact of 1 GeV/u U^{92+} ions on helium. Ionization cross sections differential in the longitudinal momentum of the recoil ion and electron emission cross sections differential in electron energy for single and double ionization were shown to closely follow those arising by exposure to an intense, ultrashort, broadband photon field.

We show here how double ionization of helium by charged particles could be classified into hard and soft collisions. We also draw attention to similarities between the double ionization of helium by charged particle impact and photoabsorption, on the basis of angular distributions of the ejected electrons.

2. Experiments

The experiments were done at the Grand Accelerator National de Ions Lourd (GANIL) with 100 MeV/u C^{6+} ions. The target was an internally cold supersonic jet of helium gas. The gas jet assembly is a part of the "Reaction Microscope" which is described elsewhere in detail [8]. Briefly, it comprises a pair of parallel ceramic plates 22 cm × 10 cm in size, which generate a uniform electric field antiparallel to the ion beam. A homogenous solenoidal magnetic field generated by two coils 1.2 m in diameter is also applied along the electric field direction. The two fields efficiently guide the ions and electrons formed in the interaction volume onto large channel plate detectors. Separation of the ion fragments is done on the basis of the flight times, and the distances of the detectors from the interaction region are arranged to achieve a time focusing geometry. Knowing the flight times and the position of arrival of the ions and electrons, combined with the accurately known and extremely homogenous extraction fields, the trajectories of the ions and electrons are reconstructed after the experiment is over. The magnetic field in the spectrometer was about 19 G, and the electric field about 5 V/cm. With this configuration, all electrons upto 20 eV kinetic energy are guided to the detector irrespective of the initial direction of their velocities, but electrons with higher energy ejected in the direction away from the detector are lost. The collection efficiency for electrons emitted transverse to the beam direction is high due to the axial magnetic field. The overall collection efficiency is about 0.5 for electrons upto 50 eV energy and better than 0.98 for the recoil ions.

3. Results

The momentum information from the experiment can be analysed in several ways, and cross sections differential in the momentum transfer can be obtained. For a comparison of charged particle-impact ionization with photoionization we note that in photoionization there is negligible momentum transfer to the target. In case of a fast charged projectile, the component of the change of the momentum of the projectile perpendicular to the direction of propagation ($q_\perp$) is significant, while the component along the direction of pro-

pogation ($q_{||}$) is small. Thus, the momentum vector $q_\perp$ plays a key role in distinghuishing between soft and hard collisions. Our analysis is based on angular distributions of the electrons in the plane transverse to the beam axis, i.e. the azimuthal plane, which contains the $q_\perp$ vector. The azimuthal angles are measured with respect to the direction of $q_\perp$.

3.1. *Separation into soft and hard collisions*

For most of the collisions analysed here, the momentum transferred is simply equal and opposite to $q_\perp$. The magnitude of $q_\perp$ is a measure of the scattering angle of the projectile, which in turn is a measure of the impact parameter. In the impact parameter formulation of a collision, it is generally accepted that an appropriate length scale for demarcating close and distant encounters is the mean target radius, a_0. This distance scale also sets the scale for separating hard and soft collisions in terms of the momentum transfer q, through the relation $q_0 \simeq \hbar/a_0$. Do we have evidence for the appropriateness of this scale?

Fig. 9 shows the electron emission patterns in the azimuthal plane for small ($q < 1.2$ a.u.) and large ($q > 1.2$ a.u.) momentum transfers. We label the more energetic electron as electron 1, and the less energetic electron as electron 2, irrespective of their order of detection. The distinction between soft and hard collisions is clearly seen from the figure. For soft collisions, both electrons show uniform distribution in the transverse plane, but for hard collisions, electron 1 is preferentially scattered opposite to $q_\perp$, i.e. along the momentum transfer direction. This sharp difference between the distributions of the two electrons indicates that electron 1 is removed by a direct encounter with the projectile, while the second is removed by an indirect process, probably providing a signature of a shakeoff.

3.2. *Comparison of soft collisions and photoionization*

For soft collisions the momentum transferred by the projectile to the target is not sufficient to impart enough kinetic energy

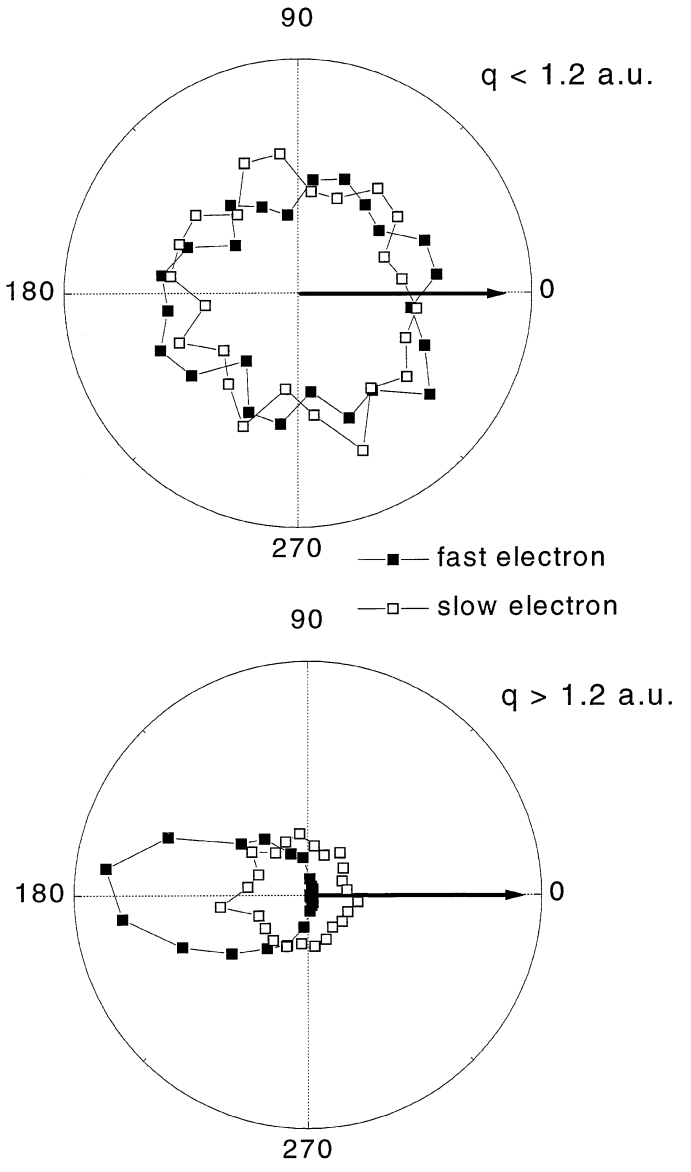

Fig. 1. Azimuthal angular distributions of the slow and fast electrons for small and large momentum transfers in the transverse plane. (a) soft collisions, $q < 1.2$ a.u. (b) hard collisions, $q > 1.2$ a.u. The arrow is along the direction of $q_\perp$.

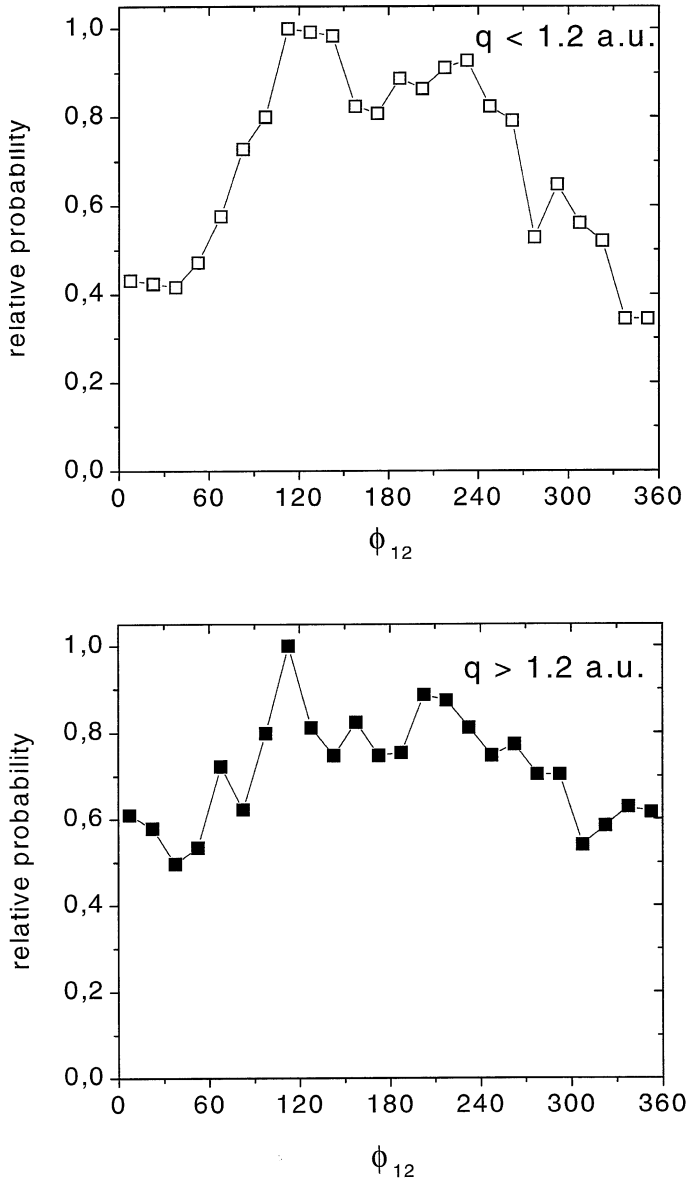

Fig. 2. The angular distribution of the azimuthal angle between the momentum vectors of the two electrons. (a) soft collisions, $q < 1.2$ a.u. (b) hard collisions, $q > 1.2$ a.u. The dip in the distribution for soft collisions at 180° is similar to the results of photoionization.

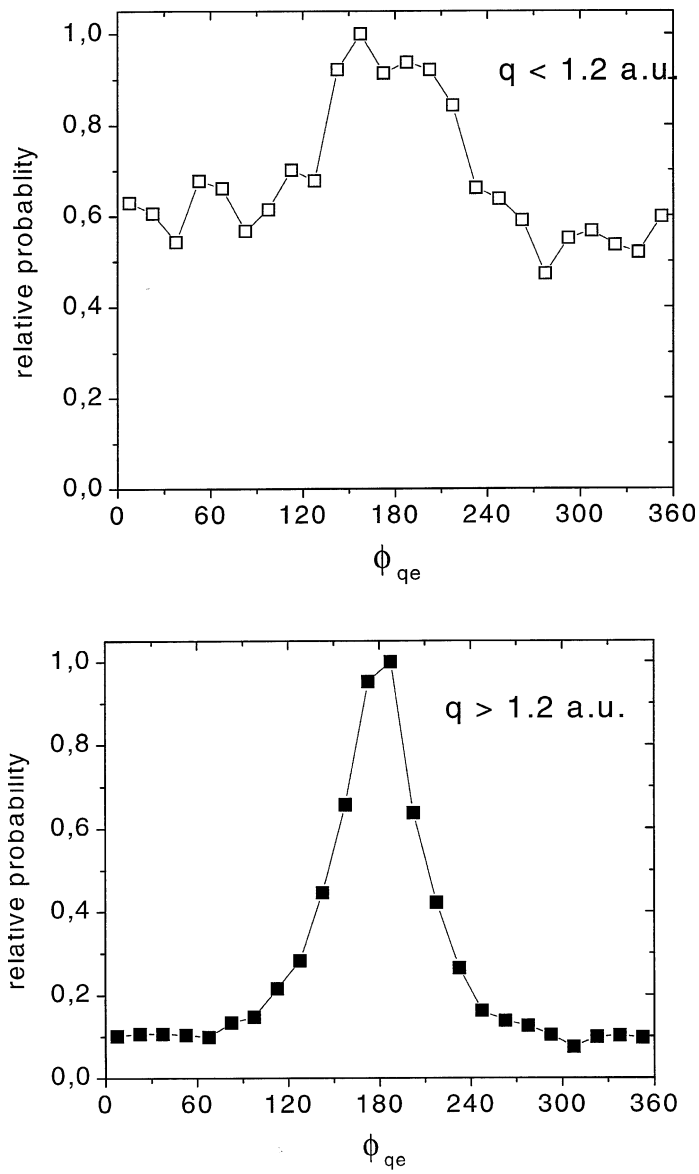

Fig. 3. The azimuthal angular distribution of the sum vector of the electron momenta. (a) soft collisions, $q < 1.2$ a.u. (b) hard collisions, $q > 1.2$ a.u.

to permit the electrons to overcome the binding energy. Thus, it may be appropriate to compare this domain with photoionization. Photoionization is characterized [9] by three main features: (a) recoil ion momentum and sum momenta of the electrons balance each other, (b) electron emission in the same direction or oppposite direction is forbidden if the electrons have equal energies (c) the sum momentum of the electrons shows a dipole pattern with respect to the polarization vector of the photon.

To simplify matters, we reduce the four-body events to three-body events by reducing the two electron coordinates to a single center of mass cordinate:

$$\boldsymbol{p}_e = \boldsymbol{p}_{e1} + \boldsymbol{p}_{e2}. \quad (1)$$

The two other vectors are $\boldsymbol{p}_R$ and $\boldsymbol{q}$. When the $\boldsymbol{q}$ vector is small, the relative orientation of the vectors $\boldsymbol{p}_e$ and $\boldsymbol{p}_R$ would be close to 180°, due to momentum conservation principles. Thus the first feature of photoionization is trivially recovered here.

The second feature, that of favoured interelectron angle can be seen in Fig. 9. The distribution shown is integrated over all electron energies for $q < q_0$, unlike the more usual energy-differential distribution for photoionization, where the rule is strictly valid. Nevertheless, we see even in the energy integral spectrum, that the favoured interelectron angles are close to 130° and 230°, and emission of the two electrons in the same or opposite directions is suppressed.

The third feature, of the dipole distribution of the $\boldsymbol{p}_e$ vector w.r.t. the $q_\perp$ vector is seen less clearly in our results (Fig. 9). The reason for this is probably that a perfect dipole pattern would be seen only if the momentum transfer were negligibly small, and from the very nature of our analysis, we cannot determine the $q_\perp$ vector accurately, if $q_\perp$ itself is small. Thus, the determination of the relative angles is inaccurate for events which would most likely be responsible for the dipole pattern.

3.3. *Hard collisions*

Apart from the change of the distribution of the angle between $\boldsymbol{p}_e$ and $\boldsymbol{p}_R$ to approximately isotropic, the most significant change occurs in the individual electron emission angles. The fast electron is invariably ejected along the momentum transfer, compensating the momentum loss of the projectile, whereas electron 2 is isotropically distributed. This is indicative of a hard, direct collision with an electron, at small impact parameters. At very small impact parameters, binary encounter with the target nucleus is also possible, and these events are indicated by a preferred antiparallel orientation of the $\boldsymbol{p}_R$ and $\boldsymbol{q}$ vectors. Hard collisions have been often thought to be similar to Compton scattering [5]. However the energy transfers in the collisions discussed here are much lower than the photon energies for which Compton scattering is important.

References

1. von Weizsäcker, C. F., Z. Phys. **88**, 612 (1934).
2. Williams, E. J., Phys. Rev. **45**, 729 (1934).
3. Bethe, H. A., Annal. Phys. **5**, 325 (1930).
4. Kim, Y. K. and Inokuti, M., Phys. Rev. A **3**, 665 (1971).
5. Andersson, L. and Burgdörfer, J., Phys. Rev. A **50**, R2810 (1994).
6. Manson, S. T. and McGuire, J. H., Phys. Rev. A **51**, 400 (1995).
7. Moshammer, R. *et al.*, Phys. Rev. Lett. **79**, 3621 (1997).
8. Moshammer, R., Unverzagt, M., Schmitt, W., Ullrich, J. and Schmidt-Böcking, H., Nucl. Instrum. Meth. B **108**, 425 (1996).
9. Schmidt, V., "Electron Spectrometry of Atoms using Synchrotron Radiation", Cambridge Monographs on Atomic, Molecular and Chemical Physics (1997).